Available online at www.sciencedirect.com
SCIENCE DIRECT®
Physics Letters B 611 (2005) 66–80
PHYSICS LETTERS B
www.elsevier.com/locate/physletb

Two-particle correlations in pp, $\bar{p}\bar{p}$ and $K^0_S K^0_S$ pairs from hadronic Z decays

ALEPH Collaboration

S. Schael

Physikalisches Institut das RWTH-Aachen, D-52056 Aachen, Germany

R. Barate, R. Brunelière, I. De Bonis, D. Decamp, C. Goy, S. Jézéquel, J.-P. Lees, F. Martin, E. Merle, M.-N. Minard, B. Pietrzyk, B. Trocmé

Laboratoire de Physique des Particules (LAPP), IN^2P^3-CNRS, F-74019 Annecy-le-Vieux cedex, France

S. Bravo, M.P. Casado, M. Chmeissani, J.M. Crespo, E. Fernandez, M. Fernandez-Bosman, Ll. Garrido [1], M. Martinez, A. Pacheco, H. Ruiz

Institut de Física d'Altes Energies, Universitat Autònoma de Barcelona, E-08193 Bellaterra (Barcelona), Spain [2]

A. Colaleo, D. Creanza, N. De Filippis, M. de Palma, G. Iaselli, G. Maggi, M. Maggi, S. Nuzzo, A. Ranieri, G. Raso [3], F. Ruggieri, G. Selvaggi, L. Silvestris, P. Tempesta, A. Tricomi [4], G. Zito

Dipartimento di Fisica, INFN Sezione di Bari, I-70126 Bari, Italy

X. Huang, J. Lin, Q. Ouyang, T. Wang, Y. Xie, R. Xu, S. Xue, J. Zhang, L. Zhang, W. Zhao

Institute of High Energy Physics, Academia Sinica, Beijing, People's Republic of China [5]

D. Abbaneo, T. Barklow [6], O. Buchmüller [6], M. Cattaneo, B. Clerbaux [7], H. Drevermann, R.W. Forty, M. Frank, F. Gianotti, J.B. Hansen, J. Harvey, D.E. Hutchcroft [8], P. Janot, B. Jost, M. Kado [9], P. Mato, A. Moutoussi, F. Ranjard, L. Rolandi, D. Schlatter, G. Sguazzoni, F. Teubert, A. Valassi, I. Videau

European Laboratory for Particle Physics (CERN), CH-1211 Geneva 23, Switzerland

0370-2693/$ – see front matter
doi:10.1016/j.physletb.2004.11.048

F. Badaud, S. Dessagne, A. Falvard [10], D. Fayolle, P. Gay, J. Jousset, B. Michel, S. Monteil, D. Pallin, J.M. Pascolo, P. Perret

Laboratoire de Physique Corpusculaire, Université Blaise Pascal, IN^{2}P^3-CNRS, Clermont-Ferrand, F-63177 Aubière, France

J.D. Hansen, J.R. Hansen, P.H. Hansen, A.C. Kraan, B.S. Nilsson

Niels Bohr Institute, 2100 Copenhagen, DK-Denmark [11]

A. Kyriakis, C. Markou, E. Simopoulou, A. Vayaki, K. Zachariadou

Nuclear Research Center Demokritos (NRCD), GR-15310 Attiki, Greece

A. Blondel [12], J.-C. Brient, F. Machefert, A. Rougé, H. Videau

Laboratoire Leprince-Ringuet, Ecole Polytechnique, IN^{2}P^3-CNRS, F-91128 Palaiseau cedex, France

V. Ciulli, E. Focardi, G. Parrini

Dipartimento di Fisica, Università di Firenze, INFN Sezione di Firenze, I-50125 Firenze, Italy

A. Antonelli, M. Antonelli, G. Bencivenni, F. Bossi, G. Capon, F. Cerutti, V. Chiarella, P. Laurelli, G. Mannocchi [13], G.P. Murtas, L. Passalacqua

Laboratori Nazionali dell'INFN (LNF-INFN), I-00044 Frascati, Italy

J. Kennedy, J.G. Lynch, P. Negus, V. O'Shea, A.S. Thompson

Department of Physics and Astronomy, University of Glasgow, Glasgow G12 8QQ, United Kingdom [14]

S. Wasserbaech

Utah Valley State College, Orem, UT 84058, USA

R. Cavanaugh [15], S. Dhamotharan [16], C. Geweniger, P. Hanke, V. Hepp, E.E. Kluge, A. Putzer, H. Stenzel, K. Tittel, M. Wunsch [17]

Kirchhoff-Institut für Physik, Universität Heidelberg, D-69120 Heidelberg, Germany [18]

R. Beuselinck, W. Cameron, G. Davies, P.J. Dornan, M. Girone [19], N. Marinelli, J. Nowell, S.A. Rutherford, J.K. Sedgbeer, J.C. Thompson [20], R. White

Department of Physics, Imperial College, London SW7 2BZ, United Kingdom [14]

V.M. Ghete, P. Girtler, E. Kneringer, D. Kuhn, G. Rudolph

Institut für Experimentalphysik, Universität Innsbruck, A-6020 Innsbruck, Austria [21]

E. Bouhova-Thacker, C.K. Bowdery, D.P. Clarke, G. Ellis, A.J. Finch, F. Foster, G. Hughes, R.W.L. Jones, M.R. Pearson, N.A. Robertson, M. Smizanska

Department of Physics, University of Lancaster, Lancaster LA1 4YB, United Kingdom [14]

O. van der Aa, C. Delaere [22], G. Leibenguth [23], V. Lemaitre [24]

Institut de Physique Nucléaire, Département de Physique, Université Catholique de Louvain, 1348 Louvain-la-Neuve, Belgium

U. Blumenschein, F. Hölldorfer, K. Jakobs, F. Kayser, K. Kleinknecht, A.-S. Müller, B. Renk, H.-G. Sander, S. Schmeling, H. Wachsmuth, C. Zeitnitz, T. Ziegler

Institut für Physik, Universität Mainz, D-55099 Mainz, Germany [18]

A. Bonissent, P. Coyle, C. Curtil, A. Ealet, D. Fouchez, P. Payre, A. Tilquin

Centre de Physique des Particules de Marseille, Université Méditerranée, IN^{2}P^3-CNRS, F-13288 Marseille, France

F. Ragusa

Dipartimento di Fisica, Università di Milano e INFN Sezione di Milano, I-20133 Milano, Italy

A. David, H. Dietl [25], G. Ganis [26], K. Hüttmann, G. Lütjens, W. Männer [25], H.-G. Moser, R. Settles, M. Villegas, G. Wolf

Max-Planck-Institut für Physik, Werner-Heisenberg-Institut, D-80805 München, Germany [18]

J. Boucrot, O. Callot, M. Davier, L. Duflot, J.-F. Grivaz, Ph. Heusse, A. Jacholkowska [27], L. Serin, J.-J. Veillet

Laboratoire de l'Accélérateur Linéaire, Université de Paris-Sud, IN^{2}P^3-CNRS, F-91898 Orsay cedex, France

P. Azzurri, G. Bagliesi, T. Boccali, L. Foà, A. Giammanco, A. Giassi, F. Ligabue, A. Messineo, F. Palla, G. Sanguinetti, A. Sciabà, P. Spagnolo, R. Tenchini, A. Venturi, P.G. Verdini

Dipartimento di Fisica dell'Università, INFN Sezione di Pisa e Scuola Normale Superiore, I-56010 Pisa, Italy

O. Awunor, G.A. Blair, G. Cowan, A. Garcia-Bellido, M.G. Green, T. Medcalf, A. Misiejuk, J.A. Strong, P. Teixeira-Dias

Department of Physics, Royal Holloway & Bedford New College, University of London, Egham, Surrey TW20 OEX, United Kingdom [14]

R.W. Clifft, T.R. Edgecock, P.R. Norton, I.R. Tomalin, J.J. Ward

Particle Physics Department, Rutherford Appleton Laboratory, Chilton, Didcot, Oxon OX11 0QX, United Kingdom [14]

B. Bloch-Devaux, D. Boumediene, P. Colas, B. Fabbro, E. Lançon, M.-C. Lemaire, E. Locci, P. Perez, J. Rander, B. Tuchming, B. Vallage

CEA, DAPNIA/Service de Physique des Particules, CE-Saclay, F-91191 Gif-sur-Yvette cedex, France [28]

A.M. Litke, G. Taylor

Institute for Particle Physics, University of California at Santa Cruz, Santa Cruz, CA 95064, USA [29]

C.N. Booth, S. Cartwright, F. Combley ✠, P.N. Hodgson, M. Lehto, L.F. Thompson

Department of Physics, University of Sheffield, Sheffield S3 7RH, United Kingdom [14]

A. Böhrer, S. Brandt, C. Grupen, J. Hess, A. Ngac, G. Prange

Fachbereich Physik, Universität Siegen, D-57068 Siegen, Germany [18]

C. Borean, G. Giannini

Dipartimento di Fisica, Università di Trieste e INFN Sezione di Trieste, I-34127 Trieste, Italy

H. He, J. Putz, J. Rothberg

Experimental Elementary Particle Physics, University of Washington, Seattle, WA 98195, USA

S.R. Armstrong, K. Berkelman, K. Cranmer, D.P.S. Ferguson, Y. Gao [30], S. González, O.J. Hayes, H. Hu, S. Jin, J. Kile, P.A. McNamara III, J. Nielsen, Y.B. Pan, J.H. von Wimmersperg-Toeller, W. Wiedenmann, J. Wu, Sau Lan Wu, X. Wu, G. Zobernig

Department of Physics, University of Wisconsin, Madison, WI 53706, USA [31]

G. Dissertori

Institute for Particle Physics, ETH Hönggerberg, 8093 Zürich, Switzerland

Received 17 August 2004; accepted 8 November 2004

Available online 1 February 2005

Editor: M. Doser

Abstract

Two-particle correlations in pp, $\bar{\mathrm{p}}\bar{\mathrm{p}}$ and $\mathrm{K}^0_\mathrm{S}\mathrm{K}^0_\mathrm{S}$ pairs have been studied in hadronic Z decays recorded at LEP with the ALEPH detector. The correlations were measured as a function of the four-momentum difference Q of the pair. For pp, $\bar{\mathrm{p}}\bar{\mathrm{p}}$ pairs a depletion of events is observed in the region $Q < 3$ GeV, and for $\mathrm{K}^0_\mathrm{S}\mathrm{K}^0_\mathrm{S}$ pairs an enhancement of events is observed in the region $Q < 0.5$ GeV. These features are consistent with expectations from Fermi–Dirac and Bose–Einstein statistics, respectively.

1. Introduction

Studies of Bose–Einstein (BE) correlations of identical bosons and of Fermi–Dirac (FD) correlations of identical fermions produced in high energy collisions provide measurements which can be interpreted in terms of the distribution of particle sources in space and time. These correlations originate from the symmetrization or antisymmetrization of the two-particle wave functions of identical particles and lead to an enhancement or a suppression of pairs of particles emitted close to each other in phase space. This effect is sensitive to the size of the source from

[1] Permanent address: Universitat de Barcelona, 08208 Barcelona, Spain.
[2] Supported by CICYT, Spain.
[3] Now at Dipartimento di Fisica e Tecnologie Relative, Università di Palermo, Palermo, Italy.
[4] Also at Dipartimento di Fisica di Catania and INFN Sezione di Catania, 95129 Catania, Italy.
[5] Supported by the National Science Foundation of China.
[6] Now at SLAC, Stanford, CA 94309, USA.
[7] Now at Institut Inter-universitaire des hautes Energies (IIHE), CP 230, Université Libre de Bruxelles, 1050 Bruxelles, Belgique.
[8] Now at Liverpool University, Liverpool L69 7ZE, United Kingdom.
[9] Now at Fermilab, PO Box 500, MS 352, Batavia, IL 60510, USA.
[10] Now at Groupe d'Astroparticules de Montpellier, Université de Montpellier II, 34095 Montpellier, France.
[11] Supported by the Danish Natural Science Research Council.
[12] Now at Departement de Physique Corpusculaire, Université de Genève, 1211 Genève 4, Switzerland.
[13] Also IFSI sezione di Torino, CNR, Italy.
[14] Supported by the UK Particle Physics and Astronomy Research Council.
[15] Now at University of Florida, Department of Physics, Gainesville, FL 32611-8440, USA.
[16] Now at BNP Paribas, 60325 Frankfurt am Mainz, Germany.
[17] Now at SAP AG, 69185 Walldorf, Germany.
[18] Supported by Bundesministerium für Bildung und Forschung, Germany.
[19] Also at CERN, 1211 Geneva 23, Switzerland.
[20] Supported by the Leverhulme Trust.
[21] Supported by the Austrian Ministry for Science and Transport.
[22] Research Fellow of the Belgium FNRS.
[23] Supported by the Federal Office for Scientific, Technical and Cultural Affairs through the Interuniversity Attraction Pole P5/27.
[24] Research Associate of the Belgium FNRS.
[25] Now at Henryk Niewodniczanski Institute of Nuclear Physics, Polish Academy of Sciences, Cracow, Poland.
[26] Now at CERN, 1211 Geneva 23, Switzerland.
[27] Also at Groupe d'Astroparticules de Montpellier, Université de Montpellier II, 34095, Montpellier, France.
[28] Supported by the Direction des Sciences de la Matière, C.E.A.
[29] Supported by the US Department of Energy, grant DE-FG03-92ER40689.
[30] Also at Department of Physics, Tsinghua University, Beijing, People's Republic of China.
[31] Supported by the US Department of Energy, grant DE-FG0295-ER40896.
✠ Deceased.

which the identical particles of similar momenta originate. A description of the theory can be found in Refs. [1–3], for example.

This Letter is a continuation of earlier studies of FD correlations in the $\Lambda\Lambda$ channel [4]. Here FD correlations are studied using a combined sample of pp, $\bar{\mathrm{p}}\bar{\mathrm{p}}$ pairs, and BE correlations using a sample of $\mathrm{K}^0_{\mathrm{S}}\mathrm{K}^0_{\mathrm{S}}$ pairs; the two samples were selected from hadronic Z decays at LEP recorded by the ALEPH detector in the years 1992–1995. A short summary of the theory of Fermi–Dirac and Bose–Einstein correlations is given in Section 2. The data selection and the results are presented in Sections 3 and 4. Conclusions follow in Section 5 along with a comparison with other measurements [4–12].

2. Theory

The strength of two-particle BE or FD correlation effects can be expressed in terms of a two-particle correlation function $C(p_1, p_2)$ defined as

$$C(p_1, p_2) = N(p_1, p_2)/N_0(p_1, p_2), \tag{1}$$

where p_1 and p_2 are the four-momenta of the particles, $N(p_1, p_2)$ is the measured differential cross section for the pairs and $N_0(p_1, p_2)$ is that of a reference sample, which is free of BE or FD correlations but otherwise identical in all aspects to the data sample. The main experimental difficulty is to define an appropriate reference sample $N_0(p_1, p_2)$ in order to determine that part of $N(p_1, p_2)$ which can be attributed to the BE or FD correlations. An example for such a reference sample is given by events generated with the JETSET 7.4 Monte Carlo program [13] where the production of hadrons is simulated without taking into account BE or FD correlation effects.

The correlation function C is usually measured as a function of the Lorentz-invariant four-momentum difference Q with $Q^2 = -(p_1 - p_2)^2$. For $Q^2 = 0$ the effects of BE and FD correlations reach their extreme values. Various parametrisations for $C(Q)$ are proposed in the literature. Here the Goldhaber parametrisation [14] multiplied by an empirical term is used

$$C(Q) = \mathcal{N}\left[1 + \beta_{\mathrm{G}} \exp\left(-R_{\mathrm{G}}^2 Q^2\right)\right] \cdot \left(1 + \alpha_1 Q + \alpha_2 Q^2\right). \tag{2}$$

The empirical term $(1 + \alpha_1 Q + \alpha_2 Q^2)$ with free parameters α_1 and α_2 accounts for long-range two-particle correlations in $C(Q)$ at high Q values and for imperfections in the Monte Carlo simulation.

The form of Eq. (2) is expected for a spherical source with a Gaussian density distribution in the rest frame of the emitted pair. The free parameters are the normalisation $\mathcal{N}$, the suppression parameter β_{G} ($|\beta_{\mathrm{G}}| \leqslant 1$) and the radius R_{G}, which can be identified with the space–time extent of the source. In two-boson systems a value of $\beta_{\mathrm{G}} = 1$ corresponds to a completely incoherent emission; $|\beta_{\mathrm{G}}|$ is expected to be different from unity if sources of different radii (for example, due to different resonance lifetimes) contribute to the emission of the pairs [15] or if the particles have non-zero spin as explained below. This parameter is also affected by experimental backgrounds such as particle misidentification.

In addition an alternative parametrisation [16]

$$C(Q) = \mathcal{N}\left[1 + \beta_{\mathrm{E}} \exp(-R_{\mathrm{E}} Q)\right] \cdot \left(1 + \alpha_1 Q + \alpha_2 Q^2\right) \tag{3}$$

is included for purposes of comparison. The form of Eq. (3) is motivated by a Laguerre-polynomial expansion of $C(Q)$ and is useful for comparing with the data in the low Q region. More details about possible parametrisations are found in [16]. The parameter R_{E} is related to the width of the Q distribution and has a meaning different from that of R_{G}; similarly the interpretation of β_{E} is different from β_{G}.

The total wave function describing the final state of two identical particles must be either symmetric (s) or antisymmetric (a) under the exchange of the two particles, depending on the spin statistics of the particles. In the

limit of plane waves (i.e., neglecting contributions from possible final state interactions) this leads to [17]

$$|\Psi_{s,a}|^2 = 1 \pm \cos\big[(p_1 - p_2)\cdot(r_1 - r_2)\big], \tag{4}$$

where s (a) corresponds to the $+$ $(-)$ sign and $r_{1,2}$ are the four-vector positions of the two particles. In the case of identical spinless bosons, Ψ_s completely describes the final state, whereas in the case of identical fermions both Ψ_s and Ψ_a can contribute.

Since the differential cross section $P_{s,a}(p_1, p_2)$ is proportional to the integral

$$\int g(r_1, r_2, p_1, p_2)|\Psi_{s,a}|^2\, dr_1\, dr_2,$$

where $g(r_1, r_2, p_1, p_2)$ describes the source intensity and the integral is taken over the relative space–time distances r_1–r_2 of the particle emission points, it follows that the correlation function $C_{s,a}(p_1, p_2)$ for the symmetric (antisymmetric) final state should show an increase (decrease) for $Q \to 0$.

For identical bosons with non-zero spin or for identical fermions, one has also to consider their spin state. For the pp, $\bar{\mathrm{p}}\bar{\mathrm{p}}$ system the total spin may be $S = 0$ or $S = 1$ with spin wave functions s_0 and s_1^i, where $i = -1, 0, 1$ are the eigenvalues of the third component of the total spin; s_0 is antisymmetric whereas the s_1^i are symmetric under the exchange of the two (anti)protons. As the total wave function for the pp, $\bar{\mathrm{p}}\bar{\mathrm{p}}$ system is antisymmetric, s_0 must be combined with Ψ_s from Eq. (3) and the s_1^i with Ψ_a to yield the antisymmetric wave functions $\Theta_0 = \Psi_s s_0$ and $\Theta_1^i = \Psi_a s_1^i$. In general both Θ_0 and the Θ_1^i can contribute to $P(p_1, p_2)$, depending on the source. However for an ensemble with statistical spin mixture in which each of the four spin states s_0 and s_1^i is emitted with the same probability, the contributions from the Θ_1^i will dominate by a factor of three and the correlation function $C(Q)$ is expected to decrease to 0.5 as Q tends to zero.

3. The ALEPH detector and data selection

The ALEPH detector and its performance are described in detail in Refs. [18,19]. This analysis relies mainly on the information from three concentric tracking detectors, a large time projection chamber (TPC) surrounding a small conventional drift chamber (ITC) and a two-layer silicon vertex detector (VDET). For each track the TPC measures up to 21 space points and up to 338 samples of its specific ionisation dE/dx. The ITC adds eight points and the VDET provides two high precision space points per track near the primary vertex. The tracking detectors are located in an axial magnetic field of 1.5 T and have a combined transverse momentum resolution of $\Delta p_\perp / p_\perp = 0.0006 p_\perp \oplus 0.005$ (with $p_\perp$ in GeV/c).

The analysis was performed on data collected at the Z peak in 1992–1995. The event sample consists of a total of 3.9 million hadronic events corresponding to an integrated luminosity of 142 pb^{-1}. A sample of 6.5 million Monte Carlo events with full detector simulation, based on JETSET 7.4, was used to generate a reference sample and to calculate the selection efficiencies. This simulated sample does not include BE or FD correlations.

Hadronic events were required to contain at least five well reconstructed tracks. Each such track had to have at least four TPC hits and a polar angle in the range $|\cos\theta| < 0.95$. The point of closest approach of the reconstructed tracks to the beam axis had to be within 10 cm of the nominal interaction point along the beam direction and within 2 cm in the plane transverse to the beam. The total energy of all tracks satisfying the above cuts was required to be greater than 10% of the centre-of-mass energy.

3.1. pp, $\bar{\mathrm{p}}\bar{\mathrm{p}}$ *selection*

Protons and antiprotons were identified using the dE/dx measurement. The simulation was used to compute a proton (antiproton) probability P

$$P(I_{\mathrm{obs}}, p) = f_{\mathrm{p}}(p) \cdot G_{\mathrm{p}}(I_{\mathrm{obs}}) \Big/ \sum_i f_i(p) \cdot G_i(I_{\mathrm{obs}}), \tag{5}$$

where the $f_i(p)$ are the momentum-dependent fractions of particles of type i = e, μ, π, K and p generated by the simulation and the G_i are the corresponding Gaussian distributions for dE/dx. These are given by

$$G_i = \exp\bigl(-\bigl(I_{\mathrm{obs}} - I^i_{\mathrm{pred}}\bigr)^2/2\sigma^2\bigr), \tag{6}$$

where I_{obs} and I^i_{pred} are the observed and the predicted dE/dx ionizations and σ is the error on I_{obs}.

The momentum spectrum for protons with momenta $p < 0.4$ GeV/c is not well described by the simulation, and in the momentum region $1.3 < p < 2.0$ GeV/c the particles of type i cannot be cleanly distinguished from each other using the dE/dx measurement. Therefore these momentum regions were excluded from the analysis. The spectrum of simulated protons in the region $0.4 < p < 1.3$ GeV/c had to be corrected to reproduce the data by giving weights to tracks generated as protons. This involved an iterative procedure as follows. After subtracting the simulated background from data and Monte Carlo, each simulated proton was weighted by the ratio of numbers of protons in data and simulation for a given momentum bin. Since this changed the probability P in Eq. (5) and therefore changed the selection, the procedure was repeated until the selection converged, which required three iterations. Finally all pairs for which the product of the two probabilities P (Eq. (5)) was greater than 70% were retained to form the sample with high purity as determined by dE/dx.

An additional step was needed to reduce background in this sample due to secondary interactions and due to decays of long-lived particles by accepting only protons produced at the primary vertex. A χ^2 probability that an individual track came from the primary vertex was defined using the impact parameter D of each track with respect to the primary vertex,

$$\chi^2 = \sum_{i,j} D_i \cdot \sigma^{-1}_{ij} \cdot D_j \tag{7}$$

with $i = r, z$ and $j = r, z$. The D_r and D_z are respectively the components of the impact parameter D perpendicular to and along the direction of the beam axis and σ_{ij} is the corresponding error matrix. Using the simulated tracks, the ratio of the χ^2 distribution for protons produced at the primary vertex to that for all protons gave a purity (due to the production vertex) as a function of χ^2. This purity is around 90% at low χ^2 and falls to zero at high χ^2. The ratio was fit to a second order polynomial in χ^2 for different momentum bins. The χ^2 for a real track could then be associated with a purity via this polynomial. Finally all particle pairs where the product of their χ^2 probabilities was greater than 70% were retained. This gave a total sample of 3526 pp, $\bar{\mathrm{p}}\bar{\mathrm{p}}$ pairs in the region $Q = 0 - 10$ GeV. The purity of true proton pairs from the primary vertex is 74% for $Q < 5$ GeV and decreases to 65% for $5 < Q < 10$ GeV, as determined by simulation.

A significant spike at $Q < 0.01$ GeV due to track splitting was removed in this analysis by requiring more that 120 dE/dx samples per track.

3.2. $\mathrm{K}^0_{\mathrm{S}}\mathrm{K}^0_{\mathrm{S}}$ *selection*

Analogous to the procedure in [4], for the selection of the neutral V^0 decays all combinations of tracks with opposite charge and with momenta higher than 150 MeV/c were examined. Both tracks had to originate from a common secondary vertex with acceptable χ^2. For the final selection and for the assignment of the different hypotheses K^0, Λ and $\bar{\Lambda}$, the most important cuts are given below.

(a) A χ^2 test of energy–momentum conservation for a given hypothesis was used, assuming that the decaying particle was produced at the primary vertex and that it decayed at a secondary vertex [20].
(b) Cuts were applied to the impact parameter D of the secondary tracks from the V^0 decay with respect to the primary vertex to remove tracks orginating at the interaction point. If D_r^i and D_z^i are respectively the components of D of a track i in the direction perpendicular to and along the direction of the beam axis and $P((D_x^i/\sigma_x^i)^2)$ $(x = r, z)$ is the χ^2 probability for one degree of freedom, then the product P_D of the four probabilities

$$P_D = \prod_{i=1}^{2} P\left(\left(D_r^i/\sigma_r^i\right)^2\right) \cdot P\left(\left(D_z^i/\sigma_z^i\right)^2\right) \tag{8}$$

for the tracks of each V^0 candidate was required to be greater than 10^{-9}.
(c) V^0 candidates with tracks having dE/dx measurements were accepted as K^0 if the χ^2 probability for the pion hypothesis for each track was > 0.005, or as Λ ($\bar{\Lambda}$) if the χ^2 probability for the pion track was > 0.005 and the probability for the p ($\bar{\mathrm{p}}$) track was > 0.01.
(d) Ambiguities between K^0_S–Λ and K^0_S–$\bar{\Lambda}$ hypotheses for a V^0 decay, which survived tests (a)–(c), were resolved by accepting the hypothesis with the best total probability P_{tot} defined as a product of the probabilities obtained from the χ^2 of tests (a) and (c).

This selection resulted in a total sample of 216 413 $K^0_S K^0_S$ pairs with 88 710 pairs in the Q range from 0 to 2 GeV. The selection efficiency for the $K^0_S K^0_S$ pairs is 27% and their purity 96% as determined by simulation studies.

4. Results

4.1. The correlation function $C(Q)$

To obtain the measured correlation function $C(Q)$ for the pp, $\bar{\mathrm{p}}\bar{\mathrm{p}}$ and $K^0_S K^0_S$ pairs two reference samples A and B were utilised:

(A) simulated pairs from the JETSET Monte Carlo which is free of FD and BE correlations, and
(B) track pairs from event mixing constructed by pairing each particle of a pair with the particles of the same type in all other events. The common coordinate system needed to associate particles produced in different events was chosen to be the three perpendicular axes defined by the eigenvalues of the sphericity tensor. The momentum of each particle in an event was calculated with respect to these axes, and Q for a mixed pair was then obtained from the components of the momenta in this system. This method removes not only possible FD or BE correlations, but also affects all other correlations, apart from the distribution of the particle momenta which is conserved by construction. In addition the phase space for the mixed samples is larger than that of the original samples. To overcome these problems the double ratio of the cross sections was used

$$C(Q) = \left(\frac{N(Q)_{\mathrm{data}}}{N(Q)_{\mathrm{data,mix}}}\right) \Big/ \left(\frac{N(Q)_{\mathrm{MC}}}{N(Q)_{\mathrm{MC,mix}}}\right). \tag{9}$$

4.2. The pp, $\bar{\mathrm{p}}\bar{\mathrm{p}}$ system

Fig. 1 shows the correlation functions $C(Q)$ of the pp, $\bar{\mathrm{p}}\bar{\mathrm{p}}$ system for the reference samples A and B described in the previous section. For the mixed sample B the ratio $N(Q)_{\mathrm{MC,mix}}/N(Q)_{\mathrm{data,mix}}$ was normalized to unity for large values of $Q > 8$ GeV. A clear decrease of $C(Q)$ for $Q < 3$ GeV is seen as expected for FD correlations. The

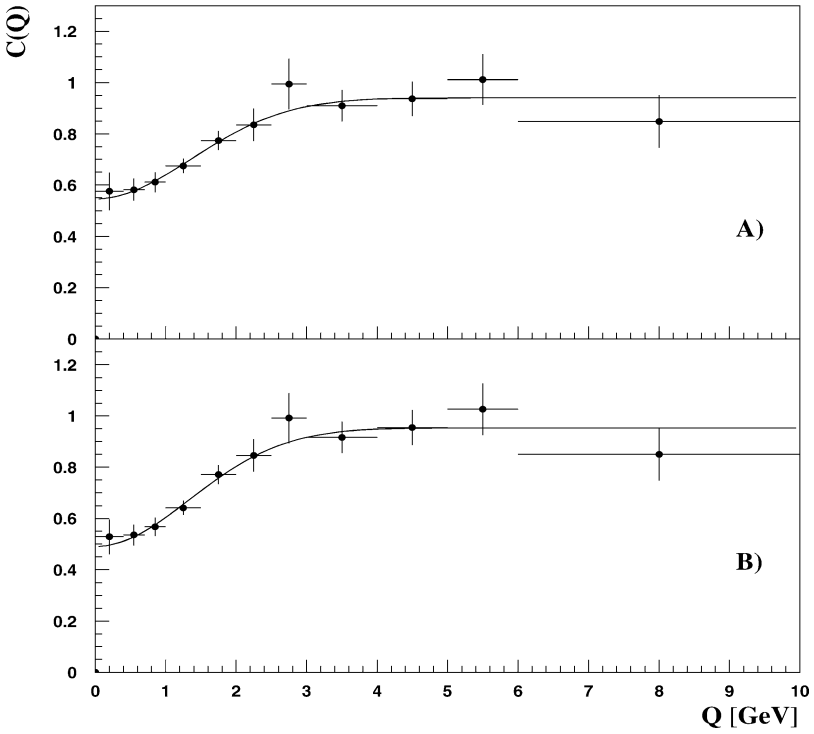

Fig. 1. Correlation function $C(Q)$ for the pp, $\bar{\mathrm{p}}\bar{\mathrm{p}}$ pairs using different reference samples: (A) Monte Carlo and (B) mixed event double ratio (see text). The solid curves represent the results of the fits using the Goldhaber parametrisation given in Eq. (2) with $\alpha_1 = 0$, $\alpha_2 = 0$ without Coulomb correction.

Table 1
The values for $\mathcal{N}$, $\beta_{\mathrm{G,E}}$ and $R_{\mathrm{G,E}}$ obtained from fits of Eqs. (2) and (3) with $\alpha_1 = 0$ and $\alpha_2 = 0$ to the correlation function $C(Q)$ for pp, $\bar{\mathrm{p}}\bar{\mathrm{p}}$ pairs for the reference samples A and B described in the text. For reference, the results including the Coulomb correction (Eq. (10)) are labelled "Coulomb". The errors in the table are statistical and without bin-to-bin correlations which are negligible in this case

Reference sample			$\mathcal{N}$	$\beta_{\mathrm{G,E}}$	$R_{\mathrm{G,E}}$ [fm]	χ^2/ndf
JETSET, A	Eq. (2)	Gaussian	0.94 ± 0.04	-0.42 ± 0.04	0.103 ± 0.015	0.34
		Coulomb	0.95 ± 0.04	-0.39 ± 0.05	0.099 ± 0.015	0.43
	Eq. (3)	Exponential	0.99 ± 0.07	-0.55 ± 0.05	0.097 ± 0.029	0.81
		Coulomb	1.00 ± 0.07	-0.51 ± 0.06	0.091 ± 0.030	0.94
Mixed events, B	Eq. (2)	Gaussian	0.95 ± 0.04	-0.49 ± 0.04	0.105 ± 0.013	0.40
		Coulomb	0.96 ± 0.04	-0.46 ± 0.04	0.102 ± 0.013	0.51
	Eq. (3)	Exponential	1.02 ± 0.07	-0.63 ± 0.05	0.096 ± 0.025	1.12
		Coulomb	1.02 ± 0.07	-0.60 ± 0.06	0.092 ± 0.030	1.28

fits to Eqs. (2) and (3) with $\alpha_1 = 0$ and $\alpha_2 = 0$ are listed in Table 1; both parametrisations give an acceptable χ^2. Non-zero values for α_1 and α_2 do not significantly improve the fits because of the limited statistics of the sample.

The contributions to the systematic uncertainty described next arise from the choice of the reference sample, Coulomb repulsion, dE/dx selection and vertex selection.

The differences in fitted values using reference samples A or B in Table 1 are small indicating that the simulation gives a reasonable description of the data. Since the reference sample B does correct for some inadequacies in the simulation as noted below, it will be used for the final results and the differences between A and B included in the systematic uncertainties.

At small Q, Coulomb repulsion between two charged protons or antiprotons is expected to alter the correlation function $C(Q)$. As this effect is not included in the simulation, its contribution was studied using the Q-dependent Gamov factor [21]

$$G(Q) = \frac{2\pi\alpha m}{Q} \cdot \frac{1}{\exp(2\pi\alpha m/Q) - 1}, \tag{10}$$

where m and α are the particle mass and the fine structure constant. It yielded a correction of 12% in the first bin ($Q < 0.4$ GeV), of 4% in the second bin ($0.4 < Q < 0.7$ GeV) and decreased to 0.3% at $Q = 8$ GeV. To estimate the effect of the Coulomb repulsion, the correlation functions for the samples A and B were refitted multiplying Eqs. (2) and (3) with the Gamov factor of Eq. (10); the results are listed for reference in Table 1. The fitted values for $R_{\mathrm{G,E}}$ and $\beta_{\mathrm{G,E}}$ obtained with the Coulomb correction agree with the uncorrected values within errors, but are all smaller than without including this effect. However, it has been pointed out that Eq. (10) may over-compensate for the final-state Coulomb interaction [22], so that the final result will be quoted without it and its effect only included in the systematic uncertainty.

In order to estimate the systematic effect due to the corrections to the simulated momentum spectrum described in Section 3, the analysis was repeated applying 50% of the estimated reweighting. For reference sample B, the differences between full and 50% reweighting are 0.01 fm for R and 0.02 for β for fits using either Eq. (2) or Eq. (3). The differences are larger for reference sample A, indicating that the event-mixing method indeed adjusts for imperfections in the simulation.

For the vertex selection described in Section 3.1, the product of vertex χ^2 probability was varied by $\pm 10\%$ around the nominal value of 70%. One-half the differences were 0.004 fm for R and 0.02 for β for either Eq. (2) or Eq. (3) and were combined with the systematic uncertainties.

The final results for $R_{\mathrm{G,E}}$ and $\beta_{\mathrm{G,E}}$ taken from the fits, with fixed $\alpha_1 = 0$ and $\alpha_2 = 0$ for sample B without Coulomb corrections and with the systematic effects described above combined in quadrature, are:
for Eq. (2)

$$R_{\mathrm{G}} = 0.11 \pm 0.01_{\mathrm{stat}} \pm 0.01_{\mathrm{sys}}\ \mathrm{fm},$$
$$\beta_{\mathrm{G}} = -0.49 \pm 0.04_{\mathrm{stat}} \pm 0.08_{\mathrm{sys}},$$

and for Eq. (3)

$$R_{\mathrm{E}} = 0.10 \pm 0.03_{\mathrm{stat}} \pm 0.02_{\mathrm{sys}}\ \mathrm{fm},$$
$$\beta_{\mathrm{E}} = -0.63 \pm 0.05_{\mathrm{stat}} \pm 0.09_{\mathrm{sys}}.$$

Within errors the correlation function $C(Q)$ is 0.5 at $Q = 0$, as expected for a statistical spin mixture in which each of the four spin states is emitted with the same probability, and electromagnetic and strong final-state interactions (FSI) in the di-nucleon system are small at threshold. The influence of FSI for nucleons could be directly studied in $\Lambda\Lambda$ final states [4] where electromagnetic interactions are absent. It turned out that FSI affects only the first Q^2 bin (< 0.4 GeV) and is small compared with the statistical errors, which are similar to those in the present Letter.

4.3. *The* $\mathrm{K^0_S K^0_S}$ *system*

In contrast to identical particle systems such as $\pi^{\pm}\pi^{\pm}$ or $\mathrm{K^{\pm}K^{\pm}}$, the symmetry property of identical particles is not automatically guaranteed for the $\mathrm{K^0_S K^0_S}$ system. This is because the $\mathrm{K^0_S K^0_S}$ system may not only originate

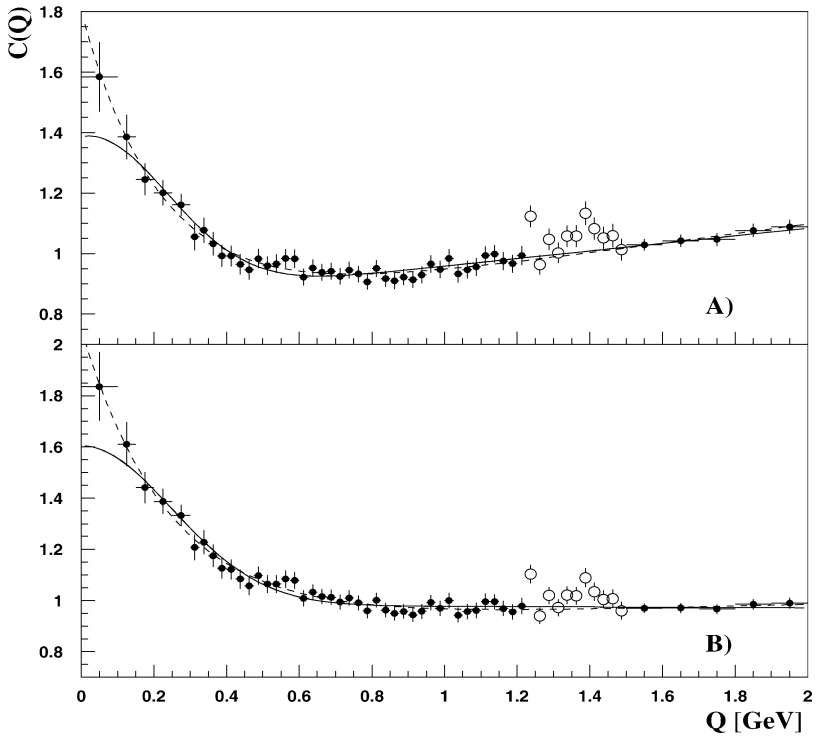

Fig. 2. Correlation function $C(Q)$ for the $K^0_S K^0_S$ pairs using different reference samples: (A) Monte Carlo simulation and (B) mixed event double ratio (see text). The curves represent the results of the fits using the Goldhaber parametrisation given in Eq. (2) (full lines) and the exponential parametrisation given in Eq. (3) (dashed lines), both with $\alpha_2 = 0$. The region affected by the $f_0(1710)$ (open circles) has been excluded from the fits.

from identical K^0K^0 and $\bar{K}^0\bar{K}^0$ pairs but also from a $K^0\bar{K}^0$ boson–antiboson system. However it has been shown in [23,24] that also in the latter case a signal from a BE-like correlation should be observed, if the background from $K^0_S K^0_L$ is small in the selected $K^0_S K^0_S$ data sample.

The measured correlation functions $C(Q)$ of the $K^0_S K^0_S$ system found for reference samples A and B are displayed in Fig. 2. One observes a clear enhancement of $C(Q)$ for values of $Q < 0.5$ GeV as expected for BE correlations. For the reference sample A one also sees a rise of $C(Q)$ for values of $Q > 0.8$ GeV (Fig. 2A) which is not seen for $C(Q)$ obtained for reference sample B (Fig. 2B). This is due to the imperfection of the simulation as shown in Fig. 3 where the ratio $R_{\mathrm{mix}} = N(Q)_{\mathrm{data,mix}}/N(Q)_{\mathrm{MC,mix}}$ is plotted as a function of Q. The ratio R_{mix} rises with Q in the whole range $0 < Q < 2$ GeV whereas it should be constant for a perfect simulation.

The region affected by the $f_0(1710)$ ($1.225 < Q < 1.5$ GeV) is not well described by the simulation, and has therefore been excluded from the fit (open circles in Fig. 2). The deviation of the fitted results by including this region are accounted for in the systematic uncertainties.

In the simulated reference sample the decay of the $f_0(980) \to K^0_S K^0_S$ was generated originally at a mass of 1.0 GeV with zero width. In the reference sample used these events were replaced by a Breit–Wigner distribution proposed by Flatté [25],

$$d\sigma/dm_{\mathrm{KK}} = N_{\mathrm{F}} \cdot \frac{m_0^2 \cdot \Gamma_{\mathrm{KK}}}{(m_0^2 - m_{\mathrm{KK}}^2)^2 + (m_0 \cdot (\Gamma_{\pi\pi} + \Gamma_{\mathrm{KK}}))^2}, \tag{11}$$

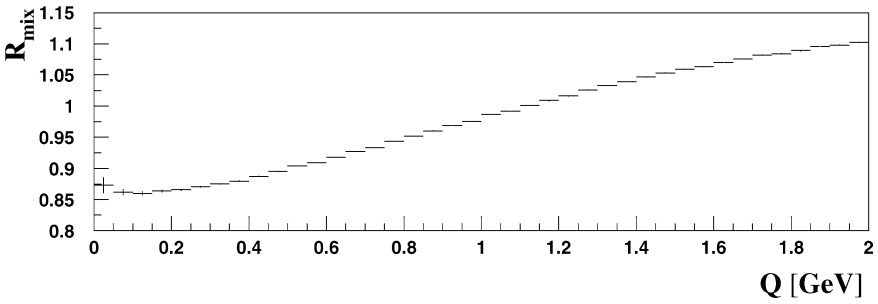

Fig. 3. The ratio $R_{\mathrm{mix}} = N(Q)_{\mathrm{data,mix}}/N(Q)_{\mathrm{MC,mix}}$ for the $\mathrm{K^0_S K^0_S}$ pairs.

Table 2
The values for α_1, α_2, $\beta_{\mathrm{G,E}}$ and $R_{\mathrm{G,E}}$ obtained from fits of Eqs. (2) and (3) to the correlation function $C(Q)$ for the $\mathrm{K^0_S K^0_S}$ pairs for reference samples A and B described in the text. The errors in the table are statistical and without bin-to-bin correlations which are negligible in this case

Reference sample		α_1	α_2	$\beta_{\mathrm{G,E}}$	$R_{\mathrm{G,E}}$ [fm]	χ^2/ndf
JETSET, A	Eq. (2)	0.15 ± 0.03	0.0 (fixed)	0.66 ± 0.06	0.62 ± 0.05	0.63
		-0.10 ± 0.09	0.09 ± 0.04	0.54 ± 0.08	0.72 ± 0.08	0.54
	Eq. (3)	0.21 ± 0.04	0.0 (fixed)	1.32 ± 0.12	0.94 ± 0.11	0.44
		0.38 ± 0.08	-0.05 ± 0.03	1.52 ± 0.14	0.88 ± 0.08	0.44
Mixed events, B	Eq. (2)	0.005 ± 0.03	0.0 (fixed)	0.63 ± 0.06	0.57 ± 0.04	0.68
		-0.27 ± 0.05	0.10 ± 0.02	0.50 ± 0.07	0.70 ± 0.07	0.52
	Eq. (3)	0.04 ± 0.03	0.0 (fixed)	1.25 ± 0.11	0.84 ± 0.10	0.43
		0.03 ± 0.06	0.004 ± 0.02	1.24 ± 0.14	0.85 ± 0.09	0.44

where m_0 is the mass of the $\mathrm{f_0}(980)$ and the widths $\Gamma_{\pi\pi}$ and Γ_{KK} are related to the coupling constants g_π and g_{K},

$$\Gamma_{\pi\pi} = g_\pi \sqrt{m^2_{\mathrm{KK}}/4 - m^2_\pi} \quad \text{and} \quad \Gamma_{\mathrm{KK}} = g_{\mathrm{K}} \sqrt{m^2_{\mathrm{KK}}/4 - m^2_{\mathrm{K}}}.$$

The normalization factor N_{F} has been adjusted to the total number of predicted $\mathrm{f_0}(980) \to \mathrm{K^0_S K^0_S}$ decays by integrating Eq. (11) in the range of $0 < m_{\mathrm{KK}} < 1.5$ GeV. The values used, $m_0 = 0.954$ GeV, $g_\pi = 0.11$ and $g_{\mathrm{K}} = 0.423$, were confirmed by the OPAL experiment [26]. The contribution of the $\mathrm{f_0}(980)$ obtained from Eq. (11) mainly affects the region of $Q < 0.1$ GeV.

The fitted values for α, β and R are shown in Table 2 for reference samples A and B. Within statistics, both Eqs. (2) and (3) result in acceptable fits to the correlation functions in the range $Q < 2$ GeV. As can be seen in Fig. 2, the exponential fits (Eq. (3)) yield a higher intercept at $Q = 0$ than the Gaussian fits (Eq. (2)) and thus result in a better description of the data in the low Q region. The results for the fitted values α_1, α_2, $\beta_{\mathrm{G,E}}$ and $R_{\mathrm{G,E}}$ are listed in Table 2 for fixed $\alpha_2 = 0$ and for α_2 as a free parameter in the fit.

It was found that other parametrisations [16] having for example cubic terms in the polynomial in Eqs. (2) and (3) gave no improvement to the fits. Distinguishing such details would require a data sample with much higher statistics than available here.

Systematic errors include the uncertainty in the choice of the reference sample (A or B) and the uncertainty of the parametrisation of $C(Q)$ (α_2 fixed or free) and are taken from Table 2. Additional contributions to the systematic errors were studied by varying the selection criteria and by removing from the fits the bin below $Q < 0.1$ GeV where the uncertainty of the reference samples is highest. These have been estimated to be 0.03 fm for R and 0.05 for β and included in the systematic uncertainties.

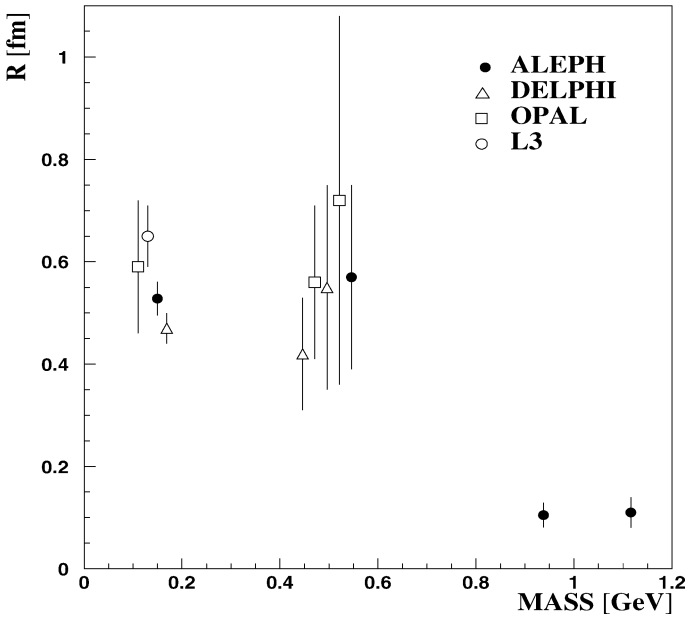

Fig. 4. Overview of results for R_G plotted as a function of particle mass. The values for R_G for the four LEP experiments have been obtained using the Goldhaber parametrisation given in Eq. (2). The results of ALEPH [4,12], DELPHI [9] and OPAL [6,11] were obtained using reference samples corresponding to B, while those for DELPHI [7], L3 [10] and OPAL [5] use reference samples corresponding to A. The errors shown are the linear sum of the statistical and the systematic errors.

The final values for $R_{G,E}$ and $\beta_{G,E}$ have been taken from fits of Eqs. (2) and (3) with fixed $\alpha_2 = 0$ using reference sample B. For this case, the result using Eq. (2) is

$$R_G = 0.57 \pm 0.04_{stat} \pm 0.14_{sys} \text{ fm},$$
$$\beta_G = 0.63 \pm 0.06_{stat} \pm 0.14_{sys},$$

and using Eq. (3) is

$$R_E = 0.84 \pm 0.10_{stat} \pm 0.10_{sys} \text{ fm},$$
$$\beta_E = 1.25 \pm 0.11_{stat} \pm 0.08_{sys}.$$

5. Conclusions

The two-particle correlation functions $C(Q)$ of the pp, $\bar{p}\bar{p}$ system and the $K^0_S K^0_S$ system have been measured as a function of the Lorentz invariant momentum difference Q. Independent of the reference sample used, $C(Q)$ shows a decrease for $Q < 3$ GeV for the pp, $\bar{p}\bar{p}$ system and an enhancement for $Q < 0.5$ GeV for the $K^0_S K^0_S$ system. If this is interpreted as a FD or BE effect, the size R_G of the sources estimated from $C(Q)$ with the Goldhaber parametrisation (Eq. (2)) are

$$R_G = 0.11 \pm 0.01_{stat} \pm 0.01_{sys} \text{ fm}$$

for the pp, $\bar{p}\bar{p}$ system, and

$$R_G = 0.57 \pm 0.04_{stat} \pm 0.14_{sys} \text{ fm}$$

for the $K^0_S K^0_S$ system.

The values for R_G are plotted in Fig. 4 together with those measured in systems of identical pions (DELPHI [9], L3 [10], OPAL [11] and ALEPH [12]), kaons (DELPHI [7], OPAL [5,6] and this measurement), protons (this measurement) and lambdas (ALEPH [4]). Only the results with reference samples corresponding to A or B as used in the present Letter have been included in this figure, in order to compare data based on the same procedure. There is indication of a dependence of R_G on the type of the particles involved, being higher for mesons than for fermions.

Acknowledgements

It is a pleasure to acknowledge our colleagues in the accelerator divisions of CERN for the excellent performance of LEP. Thanks are also due to the technical personnel of the collaborating institutions for their support in constructing and maintaining the ALEPH experiment. Those of us from non-member states thank CERN for its hospitality.

References

[1] G.I. Kopylov, M.I. Podgoretskiĭ, Sov. J. Nucl. Phys. 15 (1972) 219;
G.I. Kopylov, M.I. Podgoretskiĭ, Sov. J. Nucl. Phys. 18 (1974) 336;
G.I. Kopylov, Phys. Lett. B 50 (1974) 472.
[2] G. Cocconi, Phys. Lett. B 49 (1974) 459.
[3] R. Hanbury Brown, R.Q. Twiss, Nature 177 (1956) 27;
R. Hanbury Brown, R.Q. Twiss, Nature 178 (1956) 1046.
[4] ALEPH Collaboration, Phys. Lett. B 475 (2000) 395.
[5] OPAL Collaboration, Phys. Lett. B 298 (1993) 456.
[6] OPAL Collaboration, Eur. Phys. J. C 21 (2001) 23.
[7] DELPHI Collaboration, Phys. Lett. B 379 (1996) 330.
[8] ALEPH Collaboration, Z. Phys. C 54 (1992) 75.
[9] DELPHI Collaboration, Phys. Lett. B 286 (1992) 201.
[10] L3 Collaboration, Phys. Lett. B 540 (2002) 185.
[11] OPAL Collaboration, Phys. Lett. B 559 (2003) 131.
[12] ALEPH Collaboration, Eur. Phys. J. C 36 (2004) 147.
[13] T. Sjöstrand, et al., Comput. Phys. Commun. 135 (2001) 238.
[14] G. Goldhaber, et al., Phys. Rev. 120 (1960) 300.
[15] R. Lednický, M.I. Podgoretskiĭ, Sov. J. Nucl. Phys. 30 (1979) 432.
[16] T. Csörgö, in: R. Hwa (Ed.), Contribution to the Proceedings of the Cracow Workshop on Soft Physics and Fluctuations, Cracow, Poland, 1993, World Scientific, 1993, p. 175.
[17] B. Lörstad, Int. J. Mod. Phys. A 4 (1989) 2861;
M.G. Bowler, Z. Phys. C 29 (1985) 617.
[18] ALEPH Collaboration, Nucl. Instrum. Methods A 294 (1990) 121.
[19] ALEPH Collaboration, Nucl. Instrum. Methods A 360 (1995) 481;
ALEPH Collaboration, Phys. Lett. B 492 (2000) 275.
[20] B. Rensch, Ph.D. Thesis, Universität Heidelberg, September 1992.
[21] M. Gyulassy, S.K. Kauffmann, L.W. Wilson, Phys. Rev. C 20 (1979) 2267;
S. Pratt, Phys. Rev. D 33 (1986) 73.
[22] M.G. Bowler, OUNP-91-23, 1991;
M.G. Bowler, Phys. Lett. B 270 (1991) 69.
[23] V.L. Lyuboshits, M.I. Podgoretskiĭ, Sov. J. Nucl. Phys. 30 (1979) 407.
[24] H.J. Lipkin, Phys. Lett. B 219 (1989) 474.
[25] S.M. Flatté, Phys. Lett. B 63 (1976) 224;
S.M. Flatté, Phys. Lett. B 63 (1976) 228.
[26] B.S. Zou, D.V. Bugg, Phys. Rev. D 48 (1993) 3948;
OPAL Collaboration, Eur. Phys. J. C 4 (1998) 19.